Available online at www.sciencedirect.com
ScienceDirect
Journal of Sound and Vibration 318 (2008) 313–328
JOURNAL OF SOUND AND VIBRATION
www.elsevier.com/locate/jsvi

The effects of nonlinearity on the output frequency response of a passive engine mount

Z.K. Peng*, Z.Q. Lang

Department of Automatic Control and Systems Engineering, University of Sheffield, Mappin Street, Sheffield S1 3JD, UK

Received 30 April 2007; received in revised form 7 April 2008; accepted 10 April 2008
Handling Editor: M.P. Cartmell
Available online 12 June 2008

Abstract

In this paper, the new concept of output frequency-response function (OFRF) that was derived recently by the authors from the Volterra-series theory of nonlinear systems is briefly introduced. An effective algorithm is proposed to determine the monomials in the OFRF-based representation of the output frequency response of nonlinear systems. The results are then used to analyze the output frequency response of a passive engine mount. Important conclusions regarding the effects of system nonlinearity on the output frequency-response behaviors of the engine mount are reached via theoretical analysis and verified by simulation studies. These conclusions are of significant importance for the analysis and design of vibration isolators such as engine mounts in practice.

1. Introduction

An isolator is a device that is often inserted between a support base and a piece of equipment to reduce the vibration within the equipment. The design of isolators always presents a challenge because there are various criteria and indices, which design engineers have to take into account. Linear isolators have been widely studied in literatures where the design criteria and indices can explicitly be related to the design parameters [1–3]. Obviously, this can considerably facilitate a design process. For example, Soliman and Ismailzadeh [2] analytically linked the transmissibility of linear isolators to the optimal values of mass, stiffness, and damping ratios, and consequently related the system resonant characteristics to these parameters.

The design of engine mounts based on the principle of linear isolator designs has been reported in many recent studies. Tao et al. [4] applied the sequential quadratic programming method to select the stiffness coefficient and orientations of a marine engine mount in order to minimize the vertical force transmitted from the engine to the floor and to control the structure-borne noise. Nakhaie Jazar et al. [5] used the root mean square (rms) method to optimize damping and stiffness values for an isolator by minimizing certain cost functions related to the absolute acceleration and relative displacement. A genetic algorithm was implemented by Alkhatib et al. [6] to conduct the optimal design of a car suspension system.

*Corresponding author.
E-mail addresses: z.peng@sheffield.ac.uk (Z.K. Peng), z.lang@sheffield.ac.uk (Z.Q. Lang).

0022-460X/$ - see front matter © 2008 Elsevier Ltd. All rights reserved.
doi:10.1016/j.jsv.2008.04.016

Recently, researchers have shown more and more interests in nonlinear isolators. This is because all isolators in shock and vibration systems are inherently nonlinear [7–9], and the existence of nonlinearities has to be taken into account in designs if a better performance is to be achieved. For example, Mallik et al. [7] experimentally verified that the restoring and damping forces of elastomeric isolators have to be described using a nonlinear model. Richards and Singh [8,9] found that rubber isolators have both nonlinear damping and nonlinear stiffness. As a result of this, nonlinear isolators have been extensively studied by using both analytical and numerical approaches [10–13]. Chandra et al. [10] studied the transient responses of nonlinear, dissipative shock isolators using perturbation method and the Laplace transform. They also tried to improve the performance of a nonlinear shock isolator by comparing the behaviors of four different alternatives [11]. Popov and Sankar [12] studied the effect of nonlinear orifice-type damping on the response of a vibration isolator and found the nonlinear damping can cause a significant shift of the resonant frequency to a smaller value. Ravindra and Mallik [13] parametrically investigated the effects of various types of damping on the performance of nonlinear vibration isolators under harmonic excitations. In addition, different methods have been proposed to optimize the designs of nonlinear isolators [14–17]. Nayfeh et al. [14] proposed an optimal design method based on the concept of localized nonlinear normal modes. Royston and Singh [15] proposed an analytical framework for the optimization design of mounting systems where nonlinear effects were taken into account. Deshpande et al. [16] investigated the jump avoidance condition for the secondary suspension of a piecewise linear vibration isolation system, and used the rms method to optimize the secondary suspension within a no jump zone. Nakhaie Jazar et al. [17] studied the jump avoidance condition for the design of a nonlinear passive engine mount.

Compared with the optimization of linear isolators, the optimization of nonlinear isolators is much more complicated. This is due to the lack of an explicit analytical description for the relationship between the system nonlinearity and the system output frequency response [17]. The Volterra series is a powerful tool that can deal with a wide class of nonlinear systems [18,19] and can provide a straightforward theoretical explanation to the appearance of many *nonlinear effects* including the generation of super-harmonics and the appearance of subharmonic resonances. Most recently, the authors [20] have proved that the nonlinear system frequency responses determined by the Voltrerra-series approach is one of the solutions that can be obtained by the well-known harmonic balance method.

Based on the Volterra-series theory of nonlinear systems, the authors recently propose a new concept known as output frequency-response function (OFRF) for nonlinear systems, which can be described by a polynomial-type nonlinear differential equation model that have been widely used to model nonlinear isolators [21]. This paper is dedicated to the use of the OFRF concept to derive an explicit analytical relationship between the system output frequency response and the nonlinear characteristic parameters of a passive engine mount which has been investigated in Ref. [17]. The objectives are to analytically reveal the effect of the nonlinear characteristics of the engine mount on the system output frequency behaviors so as to facilitate the analysis and design of the engine mount-based vibration isolation system. Simulation studies are performed to verify the effectiveness and significance of the new OFRF-based analysis. Although the study focuses on a specific nonlinear passive engine mount, the approach can be easily extended to other nonlinear isolators. The work therefore provides an important basis for the analytical study and design of nonlinear isolators in the frequency domain.

The paper is organized as follows.

Section 2 provides a brief introduction to the results associated with the representation of nonlinear systems in the frequency domain. These results are then applied to the determination of the frequency domain description of the nonlinear engine mount to be investigated in the present study. Section 3 is concerned with the application of the novel OFRF concept and associated technique to the analysis of the nonlinear engine mount. Particularly, a recursive algorithm is derived to determine the monomial terms which are to be included in an OFRF representation of the output spectrum for a wide class of nonlinear systems including the engine mount system. Based on the results in Section 3, the effects of nonlinear characteristic coefficients of the engine mount on the system output frequency responses are investigated in Section 4. Important conclusions are reached, which has significant implication for the analysis and design of nonlinear isolators in the frequency domain. Finally, conclusions are given in Section 5.

2. The representation of nonlinear systems in the frequency domain

Consider the class of nonlinear systems which are stable at zero equilibrium and which can be described in the neighborhood of the equilibrium by the Volterra series

$$y(t)=\sum_{n=1}^{N}\int_{-\infty}^{\infty}\cdots\int_{-\infty}^{\infty}h_n(\tau_1,\ldots,\tau_n)\prod_{i=1}^{n}u(t-\tau_i)\,\mathrm{d}\tau_i \tag{1}$$

where $y(t)$ and $u(t)$ are the output and input of the system, $h_n(\tau_1,...,\tau_n)$ is the nth-order Volterra kernel, and N denotes the maximum order of the system nonlinearity. Lang and Billings [22] have derived an expression for the output frequency response of this class of nonlinear systems to a general input. The result is

$$\begin{cases} Y(\mathrm{j}\omega)=\sum\limits_{n=1}^{N}Y_n(\mathrm{j}\omega) \quad \text{for } \forall\omega \\ Y_n(\mathrm{j}\omega)=\frac{1/\sqrt{n}}{(2\pi)^{n-1}}\int_{\omega_1+\ldots+\omega_n=\omega}H_n(\mathrm{j}\omega_1,\ldots,\mathrm{j}\omega_n)\prod\limits_{i=1}^{n}U(\mathrm{j}\omega_i)\,\mathrm{d}\sigma_{n\omega} \end{cases} \tag{2}$$

which reveals how nonlinear mechanisms operate on the input spectra to produce the system output frequency response. In Eq. (2), $Y(\mathrm{j}\omega)$ is the spectrum of the system output, $Y_n(\mathrm{j}\omega)$ represents the nth-order output frequency response

$$H_n(\mathrm{j}\omega_1,\ldots,\mathrm{j}\omega_n)=\int_{-\infty}^{\infty}\cdots\int_{-\infty}^{\infty}h_n(\tau_1,\ldots,\tau_n)\mathrm{e}^{-(\omega_1\tau_1+,\cdots,+\omega_n\tau_n)\mathrm{j}}\mathrm{d}\tau_1\ldots\mathrm{d}\tau_n \tag{3}$$

is known as the generalized frequency-response function (GFRF) [22], and

$$\int_{\omega_1+\ldots+\omega_n=\omega}H_n(\mathrm{j}\omega_1,\ldots,\mathrm{j}\omega_n)\prod_{i=1}^{n}U(\mathrm{j}\omega_i)\,\mathrm{d}\sigma_{n\omega}$$

denotes the integration of $H_n(\mathrm{j}\omega_1,\ldots,\mathrm{j}\omega_n)\prod_{i=1}^{n}U(\mathrm{j}\omega_i)$ over the n-dimensional hyper-plane $\omega_1+\cdots+\omega_n=\omega$. Eq. (2) is a natural extension of the well-known linear relationship $Y(\mathrm{j}\omega)=H_1(\mathrm{j}\omega)U(\mathrm{j}\omega)$ to the nonlinear case.

For the polynomial-type nonlinear systems described by the following differential equation [23]:

$$\sum_{m=1}^{M}\sum_{\substack{p=0\\p+q=m}}^{m}\sum_{l_1,\ldots l_{p+q}=0}^{L}c_{pq}(l_1,\ldots,l_{p+q})\prod_{i=1}^{p}D^{l_i}y(t)\prod_{i=p+1}^{p+q}D^{l_i}u(t)=0 \tag{4}$$

where $D^l y(t)=d^l y(t)/dt^l$, M and L are the maximum degree of nonlinearity in terms of $y(t)$ and $u(t)$, and the maximum order of derivative, respectively, the GFRFs can be recursively determined using an effective algorithm as follows [23]:

$$\begin{aligned} H_n(\mathrm{j}\omega_1,\ldots,\mathrm{j}\omega_n)=&-\frac{1}{\left[\sum_{l_1=0}^{L}c_{10}(l_1)(\mathrm{j}\omega_1+\cdots+\mathrm{j}\omega_n)^{l_1}\right]}\left[\sum_{l_1,\cdots,l_n=0}^{L}c_{0n}(l_1,\ldots,l_n)(\mathrm{j}\omega_1)^{l_1}\ldots(\mathrm{j}\omega_n)^{l_n}\right.\\ &+\sum_{q=1}^{n-1}\sum_{p=1}^{n-q}\sum_{l_1,\cdots,l_n=0}^{L}c_{pq}(l_1,\ldots,l_{p+q})(\mathrm{j}\omega_{n-q+1})^{l_{p+1}}\ldots(\mathrm{j}\omega_n)^{l_{p+q}}H_{n-q,p}(\mathrm{j}\omega_1,\ldots,\mathrm{j}\omega_{n-q})\\ &\left.+\sum_{p=2}^{n}\sum_{l_1,\cdots,l_p=0}^{L}c_{p0}(l_1,\ldots,l_p)H_{np}(\mathrm{j}\omega_1,\ldots,\mathrm{j}\omega_n)\right] \end{aligned} \tag{5}$$

where

$$H_{np}(.)=\sum_{i=1}^{n-p+1}H_i(\mathrm{j}\omega_1,\ldots,\mathrm{j}\omega_i)H_{n-i,p-1}(\mathrm{j}\omega_{i+1},\ldots,\mathrm{j}\omega_n)(\mathrm{j}\omega_1+\cdots+\mathrm{j}\omega_i)^{l_p} \tag{6}$$

with

$$H_{n1}(j\omega_1,\ldots,j\omega_n) = H_n(j\omega_1,\ldots,j\omega_n)(j\omega_1+\cdots+j\omega_n)^{l_1} \tag{7}$$

Consider the specific case of a nonlinear passive engine mount as shown in Fig. 1 [17]. The motion governing equation is given by

$$m\ddot{x} + (c_1 + c_2x^2)\dot{x} + (k_1 + k_2x^2)x = -m\ddot{x}_1 \tag{8}$$

where $x = x_2 - x_1$ and $k_1 > 0$. If the base excitation is harmonic given by

$$x_1 = A\,\sin(\omega t) \tag{9}$$

then Eq. (8) can be converted to a dimensionless format as follows:

$$\ddot{y} + (\xi_1 + \xi_2 y^2)\dot{y} + (1 + \rho y^2)y = r^2\,\sin(r\tau) \tag{10}$$

where $y = x/A$, $\tau = \omega_0 t$, $\omega_0 = \sqrt{k_1/m}$, $r = \omega/\omega_0$, $\rho = A^2k_2/k_1$, $\xi_1 = c_1/\sqrt{k_1 m}$, $\xi_2 = A^2c_2/\sqrt{k_1 m}$.

It can be deduced that Eq. (10) is a specific instance of Eq. (4) with $c_{0,1}(0) = -1$, $c_{1,0}(2) = 1$, $c_{1,0}(0) = 1$, $c_{1,0}(1) = \xi_1$, $c_{3,0}(0,0,1) = \xi_2$, $c_{3,0}(0,0,0) = \rho$ else $c_{p,q}(\bullet) = 0$ and $u(\tau) = r^2\,\sin(r\tau)$.

The GFRFs up to 5th-order of system (10) can be calculated recursively using algorithm (5)–(7) to produce the results below:

$$H_1(j\omega_1) = \frac{1}{-\omega_1^2 + j\omega_1\xi_1 + 1} \tag{11}$$

$$H_2(j\omega_1, j\omega_2) = 0 \tag{12}$$

$$\begin{aligned} H_3(j\omega_1, j\omega_2, j\omega_3) = & -H_1(j(\omega_1+\omega_2+\omega_3)) \\ & \times \left[\left(\rho + \tfrac{1}{3}j\xi_2(\omega_1+\omega_2+\omega_3)\right)H_1(j\omega_1)H_1(j\omega_2)H_1(j\omega_3)\right] \end{aligned} \tag{13}$$

$$H_4(j\omega_1, j\omega_2, j\omega_3, j\omega_4) = 0 \tag{14}$$

$$\begin{aligned} H_5(j\omega_1, j\omega_2, j\omega_3, j\omega_4, j\omega_5) = & -H_1(j(\omega_1+\omega_2+\omega_3+\omega_4+\omega_5)) \\ & \times \frac{3}{10}\left[\left(\rho + \frac{1}{3}j\xi_2\sum_{L=1}^{5}\omega_L\right)\sum_{\substack{(L1,\ldots,L5)\ \text{is all} \\ \text{permutations}\ (1,\ldots,5)}} H_1(j\omega_{L1})H_1(j\omega_{L2})H_3(j\omega_{L3}, j\omega_{L4}, j\omega_{L5})\right] \end{aligned} \tag{15}$$

The GFRFs are the extension of the frequency-response function of linear systems to the nonlinear case and provide a description for the characteristics of nonlinear systems in the frequency domain.

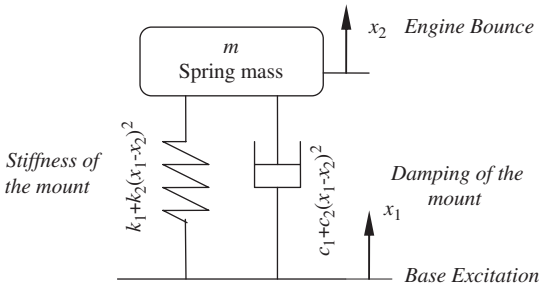

Fig. 1. Schematic of the nonlinear passive mount under a base excitation.

3. OFRF

3.1. Basic concept

The recursive algorithm (5)–(7) provides an effective approach to the determination of the GFRFs for the nonlinear systems described by Eq. (4). However, the algorithm cannot be readily used to explicitly reveal how the nonlinear characteristic coefficients of system (4) have effects on the system GFRFs. In order to address this issue, the authors proposed and proved the result in the following proposition, which reveals an explicit analytical relationship between the nonlinear characteristic coefficients in model (4) and the system GFRFs.

Proposition 1. *Denote C as the set of nonlinear characteristic parameters in model* (4). *Then, given the parameters of* $H_1(.)$ *and frequency variables* $\omega_1,\ldots,\omega_n$, *the nth order GFRF of system* (4) *can be expressed as a polynomial function of the parameters in C as* [21]

$$H_n(\mathrm{j}\omega_1,\ldots,\mathrm{j}\omega_n)=\sum_{(j_1,\ldots j_{sn})\in J_n}\Theta^{(n:j_1\ldots j_{sn})}_{\lambda_1\ldots\lambda_{sn}}(\mathrm{j}\omega_1,\ldots,\mathrm{j}\omega_n)\lambda_1^{j_1}\ldots\lambda_{sn}^{j_{sn}}\quad(n\geqslant 2)\tag{16}$$

where $\lambda_1,\ldots,\lambda_{sn}$ *are the elements in C,* $\Theta^{(n:j_1\ldots j_{sn})}_{\lambda_1\ldots\lambda_{sn}}(\mathrm{j}\omega_1,\ldots,\mathrm{j}\omega_n)$ *represents a function of* $\omega_1,\ldots,\omega_n$ *and the parameters in* $H_1(.)$, *and* J_n *is a set of* s_n *dimensional nonnegative integer vectors which contains the exponents of those monomials* $\lambda_1^{j_1}\ldots\lambda_{sn}^{j_{sn}}$ *which are present in the polynomial representation* (16).

Obviously, $\Theta^{(n:j_1\ldots j_{sn})}_{\lambda_1\ldots\lambda_{sn}}(\mathrm{j}\omega_1,\ldots,\mathrm{j}\omega_n)$ is a function that is irrelevant to the characteristic parameters of the system nonlinearity and whose structure is only dependent on the specific structure of system (4). For convenience of presentation, $\Theta^{(n:j_1\ldots j_{sn})}_{\lambda_1\ldots\lambda_{sn}}(\mathrm{j}\omega_1,\ldots,\mathrm{j}\omega_n)$ will be referred to characteristic frequency response function (CFRF) in the following. Therefore, Eq. (16) shows how the GFRFs of system (4) are related to the system nonlinear characteristic parameters $\lambda_1,\ldots,\lambda_{sn}$ and these CFRFs. For example, for the nonlinear passive engine mount (10), it is easy to derive from equations (11) to (15) that $\Theta^{(n:j_1\ldots j_{sn})}_{\lambda_1\ldots\lambda_{sn}}(\mathrm{j}\omega_1,\ldots,\mathrm{j}\omega_n)$ are

$$\Theta^{(3:1)}_{\rho}(\mathrm{j}\omega_1,\mathrm{j}\omega_2,\mathrm{j}\omega_3)=-H_1(\mathrm{j}(\omega_1+\omega_2+\omega_3))H_1(\mathrm{j}\omega_1)H_1(\mathrm{j}\omega_2)H_1(\mathrm{j}\omega_3)\tag{17}$$

$$\begin{aligned}\Theta^{(3:1)}_{\xi_2}(\mathrm{j}\omega_1,\mathrm{j}\omega_2,\mathrm{j}\omega_3)=&-\tfrac{1}{3}\mathrm{j}(\omega_1+\omega_2+\omega_3)H_1(\mathrm{j}(\omega_1+\omega_2+\omega_3))\\&\times H_1(\mathrm{j}\omega_1)H_1(\mathrm{j}\omega_2)H_1(\mathrm{j}\omega_3)\end{aligned}\tag{18}$$

$$\begin{aligned}\Theta^{(5:2)}_{\rho}(\mathrm{j}\omega_1,\ldots,j\omega_5)=&\frac{3}{10}H_1(\mathrm{j}(\omega_1+\cdots+\omega_5))\\&\times\left[\sum_{\substack{(L1,\ldots,L5)\text{ is all}\\ \text{permutations }(1,\ldots,5)}}\begin{pmatrix}H_1(\mathrm{j}\omega_{L1})H_1(\mathrm{j}\omega_{L2})H_1(\mathrm{j}\omega_{L3})H_1(\mathrm{j}\omega_{L4})\\ \times H_1(\mathrm{j}\omega_{L5})H_1(\mathrm{j}(\omega_{L3}+\omega_{L4}+\omega_{L5}))\end{pmatrix}\right]\end{aligned}\tag{19}$$

$$\begin{aligned}\Theta^{(5:1,1)}_{\rho,\xi_2}(\mathrm{j}\omega_1,\ldots,\mathrm{j}\omega_5)=&\,\mathrm{j}\frac{1}{10}H_1(\mathrm{j}(\omega_1+\cdots+\omega_5))\\&\times\left[\begin{array}{l}\displaystyle\sum_{\substack{(L1,\ldots,L5)\text{ is all}\\ \text{permutations }(1,\ldots,5)}}\begin{pmatrix}(\omega_{L3}+\omega_{L4}+\omega_{L5})H_1(j\omega_{L1})H_1(\mathrm{j}\omega_{L2})H_1(\mathrm{j}\omega_{L3})\\ H_1(\mathrm{j}\omega_{L4})H_1(\mathrm{j}\omega_{L5})H_1(\mathrm{j}(\omega_{L3}+\omega_{L4}+\omega_{L5}))\end{pmatrix}\\ \quad+(\omega_1+\cdots+\omega_5)\displaystyle\sum_{\substack{(L1,\cdots,L5)\text{ is all}\\ \text{permutations }(1,\ldots,5)}}\begin{pmatrix}H_1(\mathrm{j}\omega_{L1})H_1(\mathrm{j}\omega_{L2})H_1(j\omega_{L3})H_1(\mathrm{j}\omega_{L4})\\ H_1(\mathrm{j}\omega_{L5})H_1(\mathrm{j}(\omega_{L3}+\omega_{L4}+\omega_{L5}))\end{pmatrix}\end{array}\right]\end{aligned}\tag{20}$$

$$\Theta_{\xi_2}^{(5:2)}(j\omega_1,\cdots,j\omega_5) = -\frac{1}{30}(\omega_1+\cdots+\omega_5)H_1(j(\omega_1+\cdots+\omega_5)) \times\left[\sum_{\substack{(L1,\ldots,L5)\text{ is all}\\ \text{permutations }(1,\ldots,5)}}\begin{pmatrix}(\omega_{L3}+\omega_{L4}+\omega_{L5})H_1(j\omega_{L1})H_1(j\omega_{L2})H_1(j\omega_{L3})\\ \times H_1(j\omega_{L4})H_1(j\omega_{L5})H_1(j(\omega_{L3}+\omega_{L4}+\omega_{L5}))\end{pmatrix}\right] \tag{21}$$

and

$$H_3(j\omega_1,j\omega_2,j\omega_3) = \rho\Theta_{\rho}^{(3:1)}(j\omega_1,j\omega_2,j\omega_3) + \xi_2\Theta_{\xi_2}^{(3:1)}(j\omega_1,j\omega_2,j\omega_3) \tag{22}$$

$$H_5(j\omega_1,\ldots,j\omega_5) = \rho^2\Theta_{\rho}^{(5:2)}(j\omega_1,\ldots,j\omega_5) + \rho\xi_2\Theta_{\rho,\xi_2}^{(5:1,1)}(j\omega_1,\ldots,j\omega_5) + \xi_2^2\Theta_{\xi_2}^{(5:2)}(j\omega_1,\ldots,j\omega_5) \tag{23}$$

Substituting Eq. (16) into the second equation in Eq. (2) yields

$$Y_n(j\omega) = \sum_{(j_1,\ldots j_{s_n})\in J_n}\Phi_{\lambda_1\ldots\lambda_{s_n}}^{(n:j_1\ldots j_{s_n})}\lambda_1^{j_1}\ldots\lambda_{s_n}^{j_{s_n}} \quad (n\geqslant 2) \tag{24}$$

where

$$\Phi_{\lambda_1\ldots\lambda_{s_n}}^{(n:j_1\ldots j_{s_n})}(j\omega) = \frac{1/\sqrt{n}}{(2\pi)^{n-1}}\int_{\omega_1+,\cdots,+\omega_n=\omega}\Theta_{\lambda_1\ldots\lambda_{s_n}}^{(n:j_1\ldots j_{s_n})}(j\omega_1,\ldots,j\omega_n)\prod_{i=1}^{n}U(j\omega_i)\,d\sigma_{n\omega} \tag{25}$$

Therefore, the system output spectrum $Y(j\omega)$ can be expressed as

$$Y(j\omega) = H_1(j\omega)U(j\omega) + \sum_{n=2}^{N}\sum_{(j_1,\ldots j_{s_n})\in J_n}\Phi_{\lambda_1\ldots\lambda_{s_n}}^{(n:j_1\ldots j_{s_n})}(j\omega)\lambda_1^{j_1}\ldots\lambda_{s_n}^{j_{s_n}} \tag{26}$$

This result is referred to as the OFRF in Ref. [21]. In contrast to the general perspective of the effect of the nonlinear characteristic parameters of system (4) on the output frequency response, the OFRF reveals that given a specific input and the system linear characteristic parameters there exists a simple polynomial relationship between the output spectrum and the system nonlinear characteristic parameters.

For the nonlinear engine mount (10), when only the system nonlinearities up to fifth order are taken into account, the system OFRF can be written as

$$\begin{aligned}Y(j\omega) = {} & H_1(j\omega)U(j\omega) + \rho\Phi_{\rho}^{(3:1)}(j\omega) + \xi_2\Phi_{\xi_2}^{(3:1)}(j\omega)\\ & + \rho^2\Phi_{\rho}^{(5:2)}(j\omega) + \xi_2^2\Phi_{\xi_2}^{(5:2)}(j\omega) + \rho\xi_2\Phi_{\rho,\xi_2}^{(5:1,1)}(j\omega)\end{aligned} \tag{27}$$

which clearly reveals an explicit analytical relationship between the system nonlinear characteristic parameters ρ, ξ_2 and the output spectrum $Y(j\omega)$.

But to clearly understand how the nonlinear characteristic parameters affect the system output frequency response, the values of functions $\Phi_{\lambda_1\ldots\lambda_{s_n}}^{(n:j_1\ldots j_{s_n})}(j\omega)$ such as, e.g., $\Phi_{\rho}^{(3:1)}(j\omega)$, $\Phi_{\xi_2}^{(3:1)}(j\omega)$, $\Phi_{\rho}^{(5:2)}(j\omega)$, $\Phi_{\xi_2}^{(5:2)}(j\omega)$ and $\Phi_{\rho,\xi_2}^{(5:1,1)}(j\omega)$ for the nonlinear passive engine mount (10) have to be first determined.

3.2. Determination of the OFRF

As indicated in Eq. (26), the OFRF of nonlinear system (4) is a polynomial function of the system nonlinear characteristic parameters. The coefficients of the polynomial are the functions of the system output frequency, which are determined by the specific structure of Eq. (4), the input spectrum, and the system linear characteristic parameters. In order to use the OFRF for the system analysis and design, these coefficients have to be determined. A straightforward method is to determine the functions of frequency $\Phi_{\lambda_1\ldots\lambda_{s_n}}^{(n:j_1\ldots j_{s_n})}(j\omega)$, $\{j_1,\ldots,j_{s_n}\}\in J_n$, $n=1,\ldots,N$ directly using a symbolic computation, and then evaluate the values of these coefficients at the frequencies of interest. For example, consider the engine mount (10) subject to a sinusoidal base excitation

$$u(\tau) = r^2\sin(r\tau) \tag{28}$$

it can be deduced that the first harmonic component of the system response can be written as [19]

$$Y(\mathrm{j}r) = r^2 H_1(\mathrm{j}r) + \tfrac{3}{4} r^6 H_3(\mathrm{j}r, \mathrm{j}r, -\mathrm{j}r) + \tfrac{5}{16} r^{10} H_5(\mathrm{j}r, \mathrm{j}r, \mathrm{j}r, -\mathrm{j}r, -\mathrm{j}r) \tag{29}$$

From Eqs. (13), (15) and (29), it can be known that

$$\begin{aligned} Y(\mathrm{j}r) = {} & H_1(\mathrm{j}r)U(\mathrm{j}r) + \rho \Phi_{\rho}^{(3:1)}(\mathrm{j}r) + \xi_2 \Phi_{\xi_2}^{(3:1)}(\mathrm{j}r) \\ & + \rho^2 \Phi_{\rho}^{(5:2)}(\mathrm{j}r) + \xi_2^2 \Phi_{\xi_2}^{(5:2)}(\mathrm{j}r) + \rho \xi_2 \Phi_{\rho,\xi_2}^{(5:1,1)}(\mathrm{j}r) \end{aligned} \tag{30}$$

where

$$\Phi_{\rho}^{(3:1)}(\mathrm{j}r) = -\tfrac{3}{4} r^6 |H_1(\mathrm{j}r)|^2 (H_1(\mathrm{j}r))^2 \tag{31}$$

$$\Phi_{\xi_2}^{(3:1)}(\mathrm{j}r) = -j\tfrac{1}{4} r^7 |H_1(\mathrm{j}r)|^2 (H_1(\mathrm{j}r))^2 \tag{32}$$

$$\Phi_{\rho}^{(5:2)}(\mathrm{j}r) = \tfrac{3}{32} r^{10} |H_1(\mathrm{j}r)|^4 (H_1(\mathrm{j}r))^2 (H_1(-\mathrm{j}r) + 2H_1(\mathrm{j}r) + H_1(\mathrm{j}3r)) \tag{33}$$

$$\Phi_{\xi_2}^{(5:2)}(\mathrm{j}r) = \tfrac{1}{32} r^{12} |H_1(\mathrm{j}r)|^4 (H_1(\mathrm{j}r))^2 (H_1(-\mathrm{j}r) - 2H_1(\mathrm{j}r) - H_1(\mathrm{j}3r)) \tag{34}$$

$$\Phi_{\rho,\xi_2}^{(5:1,1)}(\mathrm{j}r) = \mathrm{j}\tfrac{1}{16} r^{11} |H_1(\mathrm{j}r)|^4 (H_1(\mathrm{j}r))^2 (6H_1(\mathrm{j}r) + 2H_1(\mathrm{j}3r)) \tag{35}$$

However, for more complicated nonlinear systems or under other type excitations, the complicated symbolic manipulations and numerical integrations involved in these operations imply that the straightforward method is not applicable in most practical situations. To solve this problem so that the OFRF concept can be used to conduct nonlinear system analysis and design in practice, a numerical algorithm has been proposed to evaluate the values of functions $\Phi_{\lambda_1 \ldots \lambda_{sn}}^{(n;j_1 \ldots j_{sn})}(\mathrm{j}\omega)$, $\{j_1, \ldots, j_{s_n}\} \in J_n$, $n = 1, \ldots, N$ at the frequencies of interest directly from system simulation or experimental test data [21]. By using the nonlinear passive engine mount (10) as an example, this algorithm will be introduced as follows.

Denote

$$\Phi^{(1:0)}(\mathrm{j}r) = r^2 H_1(\mathrm{j}r) \tag{36}$$

then Eq. (30) can be written as

$$\mathbf{Y}(\mathrm{j}r) = (1 \quad \rho \quad \xi_2 \quad \rho^2 \quad \xi_2^2 \quad \rho\xi_2)\mathbf{\Phi}(\mathrm{j}r) \tag{37}$$

where $\mathbf{\Phi}(\mathrm{j}r) = (\Phi^{(1:0)}(\mathrm{j}r), \Phi_{\rho}^{(3:1)}(\mathrm{j}r), \Phi_{\xi_2}^{(3:1)}(\mathrm{j}r), \Phi_{\rho}^{(5:2)}(\mathrm{j}r), \Phi_{\xi_2}^{(5:2)}(\mathrm{j}r), \Phi_{\rho,\xi_2}^{(5:1,1)}(\mathrm{j}r))^{\mathrm{T}}$. Assume $P \geqslant 6$ testes can be conducted by taking $(\rho, \xi_2) = (\rho_{(1)}, \xi_{2(1)}), \ldots, (\rho_{(P)}, \xi_{2(P)})$, respectively, and denote the system output frequency responses in the P tests as $Y_{(1)}(\mathrm{j}r), \ldots, Y_{(P)}(\mathrm{j}r)$.

Then

$$\bar{\mathbf{Y}}(\mathrm{j}r) = \mathbf{Q}\mathbf{\Phi}(\mathrm{j}r) \tag{38}$$

where

$$\bar{\mathbf{Y}}(\mathrm{j}r) = \begin{pmatrix} Y_{(1)}(jr) \\ \vdots \\ Y_{(P)}(jr) \end{pmatrix} \quad \text{and} \quad \mathbf{Q} = \begin{bmatrix} 1 & \rho_{(1)} & \xi_{2(1)} & \rho_{(1)}^2 & \xi_{2(1)}^2 & \rho_1 \xi_{2(1)} \\ & & & \vdots & & \\ 1 & \rho_{(P)} & \xi_{2(P)} & \rho_{(P)}^2 & \xi_{2(P)}^2 & \rho_P \xi_{2(P)} \end{bmatrix} \tag{39}$$

Therefore, $\Phi(\mathrm{j}r)$ can be determined from Eq. (38) using a least square-based approach as

$$\mathbf{\Phi}(\mathrm{j}r) = (\mathbf{Q}^{\mathrm{T}}\mathbf{Q})^{-1}\mathbf{Q}^{\mathrm{T}}\bar{\mathbf{Y}}(\mathrm{j}r) \tag{40}$$

In order to demonstrate the effectiveness of this algorithm in the analysis of the engine mount system, six sets of responses of system (10) were generated via numerical integrations using the fourth-order *Runge–Kutta*

method. These responses were obtained when $\xi_1 = 0.5$ and ξ_2,ρ were taken as (0.15, −0.15), (0.15, 0.15), (0.12, 0.0), (0.15, −0.1), (0.0, 0.0), and (0.0, 0.12), respectively. The considered range of excitation frequency was between $r = 0$ and 3.0.

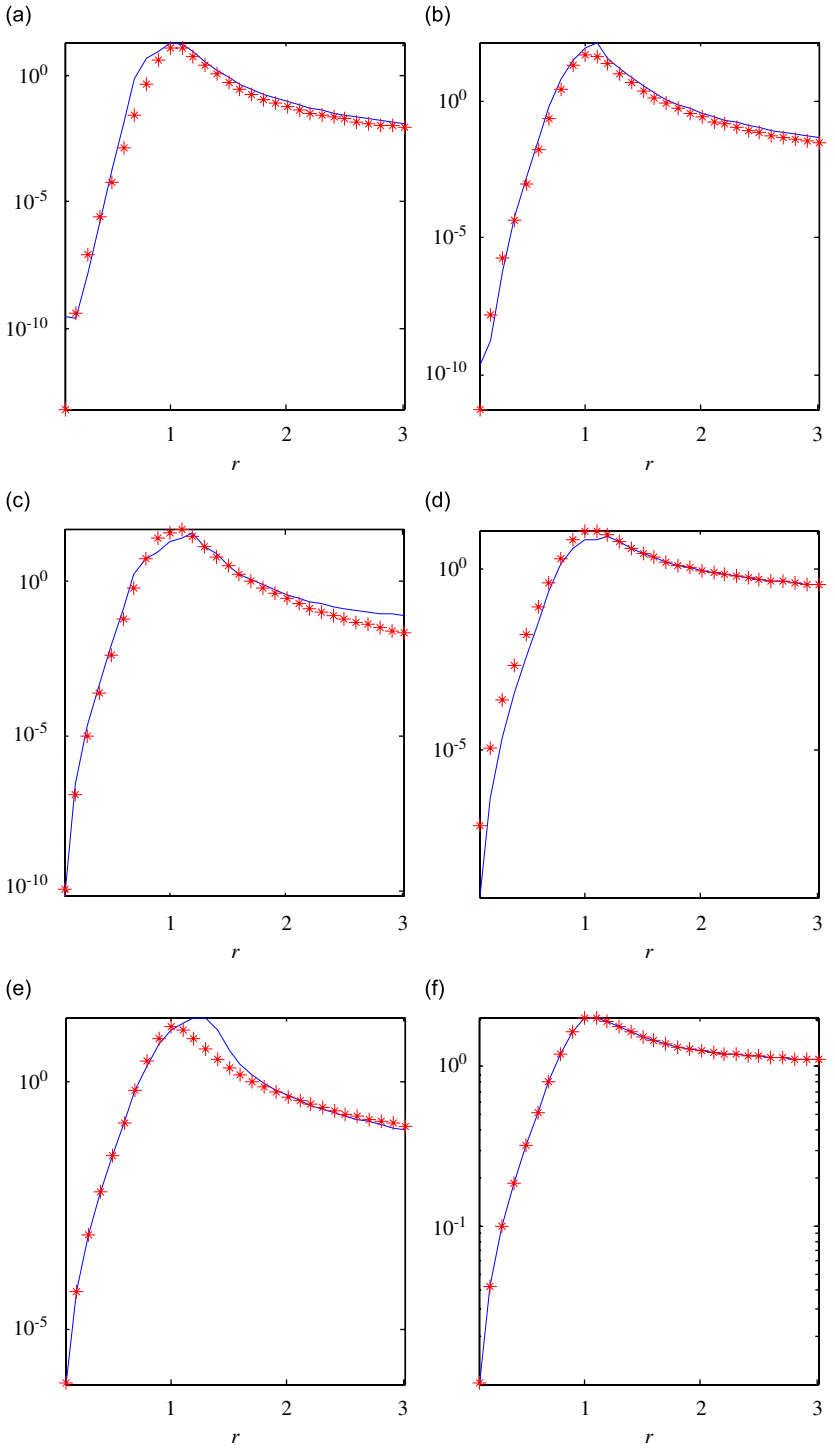

Fig. 2. A comparisons between the estimated and theoretical results of coefficients of the OFRFs: (a) $|\Phi_{\xi_2}^{(5:2)}(jr)|$, (b) $|\Phi_{\rho,\xi_2}^{(5:1,1)}(jr)|$, (c) $|\Phi_{\rho}^{(5:2)}(jr)|$, (d) $|\Phi_{\xi_2}^{(3:1)}(jr)|$, (e) $|\Phi_{\rho}^{(3:1)}(jr)|$, (f) $|\Phi^{(1:0)}(jr)|$ (solid line: estimated; asterisk: theoretical).

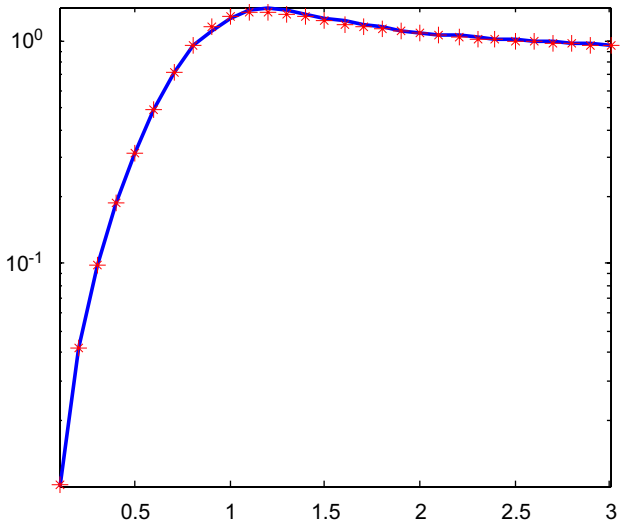

Fig. 3. The OFRF predicted (solid) and numerically calculated (asterisk) responses of system (10) when $\xi_2 = 0.2$ and $\rho = 0.2$.

From the responses of system (10) thus generated, $\Phi(\mathrm{j}r)$ was evaluated using Eq. (40). A comparison between the estimated results and the theoretical results calculated using equations (31)–(35) is shown in Fig. 2. It can be seen that, basically, the estimated results match the theoretical results well. The small deviations are mainly introduced by the truncation of the Volterra-series representation.

Using the estimated OFRF, the frequency response of system (10) under $\xi_2 = 0.2$ and $\rho = 0.2$ was predicted from Eq. (30). The predicted frequency response is given in Fig. 3 together with the response numerically calculated using the *Runge–Kutta* method. It can be seen that the OFRF-predicted frequency-response matches the real response very well.

3.3. Determination of the monomials $\lambda_1^{j_1} \dots \lambda_{s_n}^{j_{s_n}}$ in the OFRF representation of the output spectrum of nonlinear systems

The OFRF reveals a simple polynomial relationship between the nonlinear characteristic parameters and the output frequency response for nonlinear systems described by Eq. (4). In order to use the numerical algorithm in Section 3.2 to determine the OFRFs, the information about what monomials are included in Eq. (26) should be known a priori. From Eqs. (5) to (7), a recursive algorithm can be derived to determine the monomials which have to be included in an OFRF representation of the output frequency response of the nonlinear systems as below.

Denote the set of all the monomials involved in the representation of $Y_n(\mathrm{j}\omega)$ given by Eq. (16) as $\mathbf{M}_n$, and $\mathbf{M}_1 = [1]$, then $\mathbf{M}_n$ can be determined as

$$\mathbf{M}_n = \left[\bigcup_{l_1,\dots,l_n=0}^{L} [c_{0n}(l_1,\dots,l_n)]\right] \cup \left[\bigcup_{q=1}^{n-1}\bigcup_{p=1}^{n-q}\bigcup_{l_1,\dots,l_n=0}^{L} \left([c_{pq}(l_1,\dots,l_{p+q})] \otimes \mathbf{M}_{n-q,p}\right)\right] \cup \left[\bigcup_{p=2}^{n}\bigcup_{l_1,\dots,l_p=0}^{L} \left([c_{p0}(l_1,\cdots,l_p)] \otimes \mathbf{M}_{np}\right)\right] \tag{41}$$

where $\otimes$ is the Kronecker product, and

$$\mathbf{M}_{np} = \bigcup_{i=1}^{n-p+1} (\mathbf{M}_i \otimes \mathbf{M}_{n-i,p-1}) \quad \text{and} \quad \mathbf{M}_{n1} = \mathbf{M}_n \tag{42}$$

Apparently, the set of the monomials in Eq. (24) can be expressed as

$$\bar{\mathbf{M}}_N = \bigcup_{n=1}^{N} \mathbf{M}_n \tag{43}$$

It can be observed that the algorithm defined by Eqs. (41)–(43) has a form similar to Eqs. (5) and (6). The proof of this algorithm is therefore straightforward. Its effectiveness can be demonstrated using the nonlinear mount (10) as an example as follows.

Applying the algorithm to system (10) up to the seventh-order yields

$$\mathbf{M}_2 = \text{Null}$$
$$\mathbf{M}_3 = [[\xi_2] \otimes [1]] \cup [[\rho] \otimes [1]] = [\xi_2 \quad \rho]$$

$$\mathbf{M}_4 = \text{Null}$$
$$\mathbf{M}_5 = [[\xi_2] \otimes \mathbf{M}_3] \cup [[\rho] \otimes \mathbf{M}_3] = \begin{bmatrix} \xi_2^2 & \xi_2\rho & \rho^2 \end{bmatrix}$$

$$\mathbf{M}_6 = \text{Null}$$
$$\mathbf{M}_7 = [[\xi_2] \otimes \mathbf{M}_5] \cup [[\rho] \otimes \mathbf{M}_5] \cup [[\xi_2] \otimes \mathbf{M}_3 \otimes \mathbf{M}_3] \cup [[\rho] \otimes \mathbf{M}_3 \otimes \mathbf{M}_3]$$
$$= \begin{bmatrix} \xi_2^3 & \xi_2^2\rho & \xi_2\rho^2 & \rho^3 \end{bmatrix}$$

Therefore,

$$\bar{\mathbf{M}}_5 = \bigcup_{n=1}^{5} \mathbf{M}_n = \begin{bmatrix} \xi_2^2 & \xi_2\rho & \rho^2 & \xi_2 & \rho & 1 \end{bmatrix}$$

$$\bar{\mathbf{M}}_7 = \bigcup_{n=1}^{7} \mathbf{M}_n = \begin{bmatrix} \xi_2^3 & \xi_2^2\rho & \xi_2\rho^2 & \rho^3 & \xi_2^2 & \xi_2\rho & \rho^2 & \xi_2 & \rho & 1 \end{bmatrix}$$

Clearly, $\bar{\mathbf{M}}_5$ are the parameter vector used in the OFRF of system (10) given by Eq. (37). Algorithm (41)–(43) can be easily implemented using a symbolic operation method. The algorithm therefore provides a convenient way to determine the monomials involved in the OFRF representation of the output frequency response of nonlinear systems.

4. The effects of system nonlinearity on the output frequency responses

In this section, the effects of nonlinear damping characteristic parameter ξ_2 and nonlinear stiffness characteristic parameter ρ on the output frequency response of the passive engine mount (10) are studied using the OFRF concept. The focus is to investigate how the parameters ξ_2 and ρ affect the first harmonic component of the system output frequency response.

When up to third-order system nonlinearities is taken into account, the OFRF of system (10) can be obtained from (30) as

$$Y(\mathrm{j}r) \approx r^2 H_1(\mathrm{j}r)[1 - \varepsilon(3\rho + \mathrm{j}\xi_2 r)H_1(\mathrm{j}r)] \tag{44}$$

where $\varepsilon = \frac{1}{4}r^4|H_1(\mathrm{j}r)|^2$. Substituting Eq. (11) into Eq. (44) yields

$$Y(\mathrm{j}r) \approx r^2 H_1(\mathrm{j}r)\left[1 - \frac{\varepsilon}{\sqrt{(1-r^2)^2 + (r\xi_1)^2}}(3\rho + \mathrm{j}\xi_2 r)(1 - r^2 - \mathrm{j}r\xi_1)\right]$$
$$= r^2 H_1(\mathrm{j}r)(A - \mathrm{j}B) \tag{45}$$

where

$$A = 1 - 3\rho\mu(1-r^2) - \xi_2\mu\xi_1 r^2, \quad B = \mu r(-3\rho\xi_1 + \xi_2(1-r^2)), \quad \mu = \frac{\varepsilon}{\sqrt{(1-r^2)^2 + (r\xi_1)^2}}$$

Consider the cases where ξ_2 and ρ are varied within the range of [0.0, 0.2] and $\xi_1 = 0.5$. The analysis of the effect of ξ_2 and ρ on the output frequency response of the nonlinear engine mount (10) is conducted in the three situations of $r<1.0$, $r>1.0$, and $r = 1.0$, respectively.

Case 1: ($r<1.0$). In this case, the engine mount is working in the frequency range below its resonant frequency. It is not difficult to know that, over the considered range of values of ρ and ξ_2, B is much smaller than A in amplitude. Therefore, only the effect of A on $Y(\mathrm{j}r)$ is considered. Obviously, A monotonically decreases when either ρ or ξ_2 increases. Therefore, the first harmonic component of the frequency response of the nonlinear mount (10) can be reduced by increasing either ρ or ξ_2. Moreover, when $r^2<3/3.5$:

$$3\mu(1-r^2) > \mu\xi_1 r^2 \tag{46}$$

the effect of ρ is more significant than that of ξ_2 in reducing the amplitude of the first harmonic component of $Y(\mathrm{j}r)$. Fig. 4 shows the simulation results obtained using the fourth-order *Runge–Kutta* method when $r = 0.8$, and ξ_2, ρ are varied within the range of [0.0, 0.2]. From Fig. 4, it can be clearly seen that the amplitudes of the first harmonic component decrease with the increase of ξ_2 and ρ, and the effect of ρ on this decrease is more significant than the effect of ξ_2. These observations are exactly consistent with the above OFRF-based analysis.

Case 2: ($r > 1.0$). In this case, the engine mount works in the frequency range above its resonant frequency. It can be known that, over the considered range of ρ and ξ_2, A monotonically decreases with the increase of ξ_2 but increases with the increase of ρ. Meanwhile, the absolute value of B monotonically decreases with the increase of both ρ and ξ_2. Therefore, it can be predicted that, when the nonlinear mount works over the frequency range above the resonant frequency, the first harmonic component increases with the increase of ρ. Also because the value of B is much smaller than A, the effects of ρ and ξ_2 on A is the main effect. Therefore, it can be known that the amplitude of the first harmonic component can be reduced by a increase of ξ_2. Fig. 5 shows the simulation results obtained using the fourth-order *Runge–Kutta* method when $r = 2.0$, and ξ_2,ρ are varied within the range of [0.0, 0.2]. The results clearly show that the amplitudes of the first harmonic component decrease with the increase of ξ_2, but increase with the increase of ρ. These observations are again consistent with the OFRF-based analysis results.

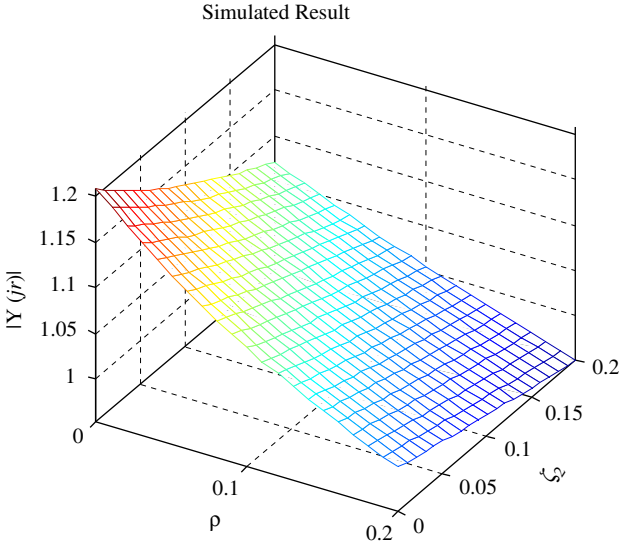

Fig. 4. The modulus of the first harmonic component of system (10) obtained using the *Runge–Kutta* method ($r = 0.8$, $\xi_1 = 0.5$).

Case 3: ($r = 1.0$). In this case, the engine mount works at the resonant frequency, and A and B can be simplified as

$$A = 1 - \xi_2 \mu \xi_1 \quad \text{and} \quad B = -3\rho r \xi_1 \mu \tag{47}$$

Obviously, A monotonically decreases with the increase of ξ_2 while the absolute value of B monotonically increase with the increase of ρ. Because of this, the amplitude of the first harmonic component of the output frequency response of system (10) should increase with the increase of ρ but decrease with the increase of ξ_2. However, the simulation results in Fig. 6 show that the amplitude of the first harmonic component monotonically decreases with an increase of both ρ and ξ_2. The inconsistency between the analysis and simulation results is due to the fact that, when working at the resonant frequency, the behavior of the

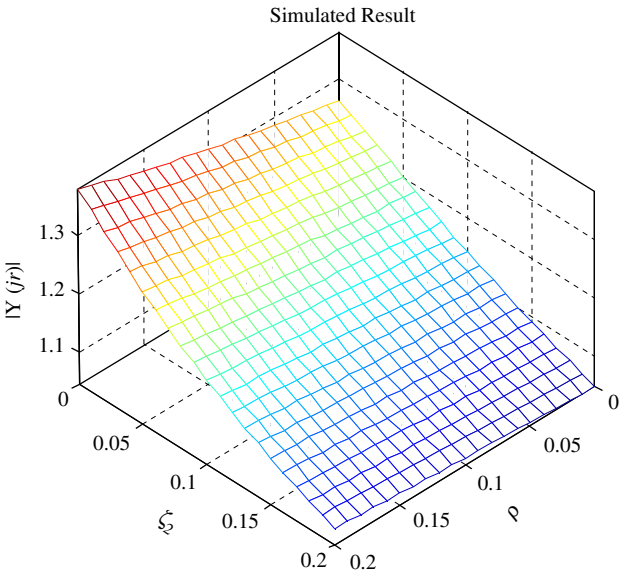

Fig. 5. The modulus of first harmonic component of system (10) obtained using the *Runge–Kutta* method ($r = 2.0$, $\xi_1 = 0.5$).

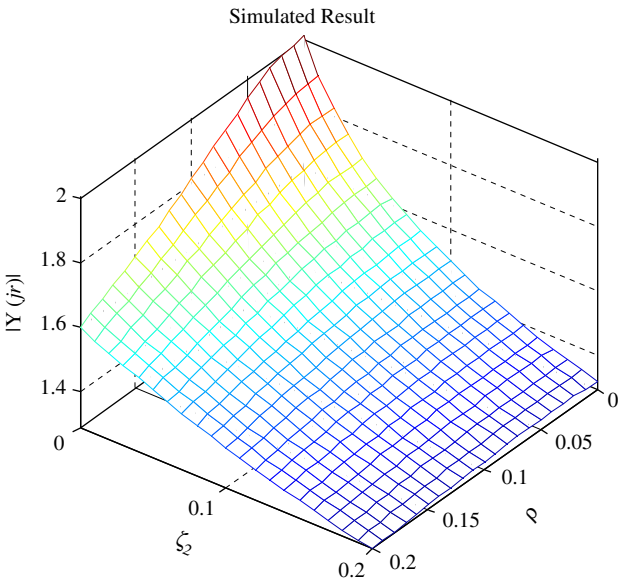

Fig. 6. The modulus of first harmonic component of system (10) obtained using the *Runge–Kutta* method ($r = 1.0$, $\xi_1 = 0.5$).

nonlinear mount (10) is considerably nonlinear but the contributions from higher order system nonlinearities were ignored in the OFRF-based analysis.

If the contribution of $\Phi_{\rho}^{(5:2)}(\mathrm{j}r)$, $\Phi_{\xi_2}^{(5:2)}(\mathrm{j}r)$ and $\Phi_{\rho,\xi_2}^{(5:1,1)}(\mathrm{j}r)$ is taken into account in the OFRF representation of the output spectrum of system (10), the first harmonic component of the system output frequency response can be described as

$$Y(\mathrm{j}r) \approx r^2 H_1(\mathrm{j}r) \times \left[1 - \left(\varepsilon(3\rho + \mathrm{j}\xi_2 r) - \delta\begin{pmatrix} 3\rho^2(H_1(-\mathrm{j}r) + 2H_1(\mathrm{j}r) + H_1(\mathrm{j}3r)) \\ +\xi_2 r^2(H_1(-\mathrm{j}r) - 2H_1(\mathrm{j}r) - H_1(\mathrm{j}3r)) \\ +\mathrm{j}2r\xi_2\rho(6H_1(\mathrm{j}r) + 2H_1(\mathrm{j}3r)) \end{pmatrix}\right) H_1(\mathrm{j}r)\right] \tag{48}$$

where $\delta = \frac{1}{32}r^8|H_1(\mathrm{j}r)|^4$. At $r = 1$, compared with $H_1(\mathrm{j}r)$, $H_1(\mathrm{j}3r)$ is ignorable. Eq. (48) can be simplified to be

$$\begin{aligned} Y(\mathrm{j}r) &\approx -j\frac{1}{\xi_1}\left[1 + \left(\varepsilon(\mathrm{j}3\rho - \xi_2) - \delta\frac{1}{\xi_1}(3\rho^2 - 3\xi_2^2 + \mathrm{j}12\xi_2\rho)\right)\frac{1}{\xi_1}\right] \\ &= \bar{B} - \mathrm{j}\bar{A} \end{aligned} \tag{49}$$

where

$$\bar{A} = \frac{1}{\xi_1}\left[1 - \varepsilon\frac{\xi_2}{\xi_1} - \frac{\delta}{\xi_1^2}(3\rho^2 - 3\xi_2^2)\right] \quad \text{and} \quad \bar{B} = 3\frac{\rho}{\xi_1}\left(\frac{\varepsilon}{\xi_1} - 4\frac{\delta}{\xi_1^2}\xi_2\right)$$

Obviously, at the considered range of ρ and ξ_2, both A and B monotonically decrease with ξ_2. This implies that, when the nonlinear mount operates at the resonant frequency, the first harmonic component of the output frequency response can be reduced by an increase of ξ_2. However, the situation for ρ is relatively complicated. It can be seen that an increase of ρ can make A decrease but B increase and, when $\rho = 0$, B is close to zero. The imaginary and real parts of the simulation results in Fig. 6 are separately shown in Fig. 7, which indicate clearly that both A and B monotonically decrease with the increase of ξ_2, and A decreases with the increase of ρ while B monotonically increases with the increase of ρ. Moreover, the value of B is close to zero at $\rho = 0$. So, by taking into account of the contribution of the fifth order nonlinearity in the OFRF-based analysis, the behavior of the nonlinear mount working at the resonant frequency has been correctly predicted. Moreover, it can be seen that an increase of ξ_2 is more effective than an increase of ρ in suppressing the amplitude of the first harmonic component.

It has to be pointed out here that, due to the strong nonlinear behavior of the nonlinear mount at the resonant frequency, Eq. (49) can only provide a qualitative analysis and prediction for the system output frequency response.

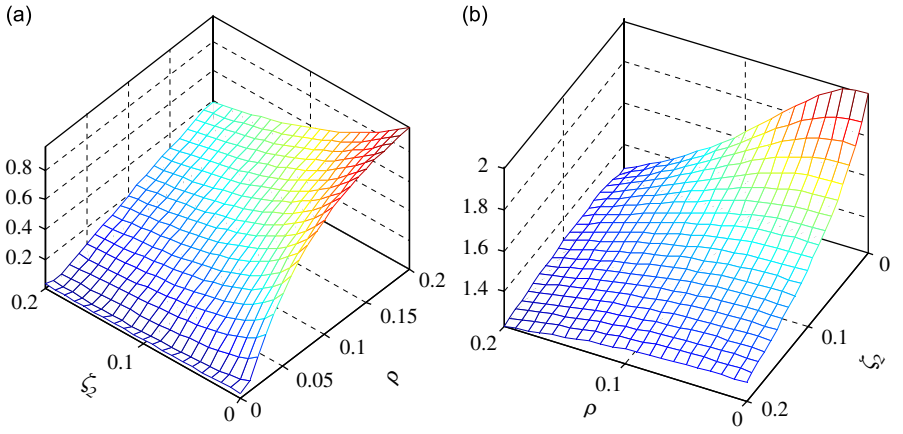

Fig. 7. The real (a) and imaginary (b) parts of the simulation results in Fig. 6.

The analysis results for the nonlinear mount (10) working at three different conditions can be summarized as below:

(1) When the nonlinear mount (10) works over a frequency range below the resonant frequency, an increase in either the nonlinear damping or the nonlinear stiffness can all reduce the amplitude of the first harmonic component of the system output frequency response; but the increase of the nonlinear stiffness is more effective in terms of suppressing the first harmonic component.
(2) When the nonlinear mount (10) works over a frequency range above the resonant frequency, an increase of the nonlinear damping can reduce the amplitude of the first harmonic component of the system output frequency response; but the effect of an increase of the nonlinear stiffness is just the opposite.
(3) When the nonlinear mount (10) works at the resonant frequency, an increase of the nonlinear damping or the nonlinear stiffness rate can all reduce the amplitude of the first harmonic component of the system output frequency response; but the increase of the nonlinear damping is more effective in terms of suppressing the first harmonic component.

These conclusions are of significant importance in the analysis and design of the nonlinear passive engine mount (10), and can be regarded as a guideline for the design or selection of mounts. For example, if a mount works over the frequency region below the resonant frequency, the guideline indicates that the mount should have a strong nonlinear stiffness. If a mount works over a frequency region above the resonant frequency, the guideline shows that the mount should have a strong nonlinear damping but a weak nonlinear stiffness.

It has to be pointed out that the Volterra series truncated at the third or fifth order has been used, respectively, in the above case studies. The analysis using an OFRF based on the third-order Volterra-series truncation produces a reasonable analysis result apart from the effect of ρ on the output spectrum. However, an improvement is obviously achieved using an OFRF based on the fifth-order Volterra-series truncation and correct results are obtained. This demonstrates that provided a sufficiently higher order Volterra-series truncation is used in the OFRF representation for the system output frequency response, correct analyses for the effects of system nonlinear characteristic parameters on the output spectrum can be achieved.

In normal working conditions of most practical systems, experiences indicate that the Volterra series is usually able to describe basic system behavior. In such circumstances, the maximum order of system nonlinearity that needs to be considered in an OFRF representation depends on the accuracy required for the OFRF-based analysis, and the numerical approach developed in the author's previous work [24] can be used to provide a sufficient condition regarding the maximum order required in the system Volterra-series representation. In addition, for many specific cases including the case of the well-known Duffing oscillator, great efforts [25–31] have been made to theoretically address the issues associated with the truncated Volterra-series-based system representations. In such specific cases, these theoretical results can be used to analytically determine the maximum order of system nonlinearity in the system's Volterra-series representation.

5. Conclusions and remarks

In this paper, the new OFRF concept and associated methods have been briefly introduced. An effective algorithm has been proposed to determine the monomials involved in the OFRF representation of the output frequency response of nonlinear systems. The OFRF-based approach is then used to analyze the effects of the nonlinear characteristic parameters of a passive engine mount on the output frequency response. Important conclusions have been obtained and validated using simulation studies. These results are of significant importance in the analysis and design of nonlinear passive engine mounts, and can be used as a guideline for the design and selection of mounts or isolators in engineering applications. It is worth pointing out that the approach proposed in this paper can be extended to multidegree of freedom (mdof) Systems. It has been observed that the OFRF of mdof systems can analytically link the system output spectrum to the characteristic parameters of nonlinear springs and/or nonlinear dampers so as to considerably facilitate the system analysis and design. The authors are currently working on these ideas. The results will be reported in future publications.

Acknowledgments

The authors gratefully acknowledge the support of the Engineering and Physical Science Research Council, UK for this work, and wish to express their thanks to the referees for helpful comments.

References

[1] C.E. Crede, *Vibration and Shock Isolation*, Wiley, New York, 1951.
[2] J.I. Soliman, E. Ismailzadeh, Optimization of unidirectional viscous damped vibration isolation system (for airborne equipment protection), *Journal of Sound and Vibration* 36 (1974) 527–539.
[3] J.C. Snowdon, Vibration isolation use and characterization, *Journal of the Acoustical Society of America* 66 (1979) 1245–1279.
[4] J.S. Tao, G.R. Liu, K.Y. Lam, Design optimization of marine engine-mount system, *Journal of Sound and Vibration* 235 (2000) 477–494.
[5] G. Nakhaie Jazar, A. Narimani, M.F. Golnaraghi, D.A. Swanson, Practical frequency and time optimal design of passive linear vibration isolation mounts, *Vehicle System Dynamics* 39 (2003) 437–466.
[6] R. Alkhatib, G. Nakhaie Jazar, M.F. Golnaraghi, Optimal design of passive linear suspension using genetic algorithm, *Journal of Sound and Vibration* 275 (2004) 665–691.
[7] A.K. Mallik, V. Kher, M. Puri, H. Hatwal, On the modelling of non-linear elastomeric vibration isolators, *Journal of Sound and Vibration* 219 (1999) 239–253.
[8] C.M. Richards, R. Singh, Experimental characterization of nonlinear rubber isolators in a multi-degree-of-freedom system configuration, *Journal of the Acoustical Society of America* 106 (1999) 2178.
[9] C.M. Richards, R. Singh, Characterization of rubber isolator non-linearities in the context of single and multi-degree-of-freedom experimental systems, *Journal of Sound and Vibration* 247 (2001) 807–834.
[10] N. Chandra Shekhar, H. Hatwal, A.K. Mallik, Response of non-linear dissipative shock isolators, *Journal of Sound and Vibration* 214 (1998) 589–603.
[11] N. Chandra Shekhar, H. Hatwal, A.K. Mallik, Performance of non-linear isolators and absorbers to shock excitations, *Journal of Sound and Vibration* 227 (1999) 293–307.
[12] G. Popov, S. Sankar, Modelling and analysis of non-linear orifice type damping in vibration isolators, *Journal of Sound and Vibration* 183 (1995) 751–764.
[13] B. Ravindra, A.K. Mallik, Performance of non-linear vibration isolators under harmonic excitation, *Journal of Sound and Vibration* 170 (1994) 325–337.
[14] T.A. Nayfeh, E. Emaci, A.F. Vakakis, Application of nonlinear localization to the optimization of a vibration isolation system, *AIAA Journal* 35 (1997) 1378–1386.
[15] T.J. Royston, R. Singh, Optimization of passive and active non-linear vibration mounting systems based on vibratory power transmission, *Journal of Sound and Vibration* 194 (1996) 295–316.
[16] S. Deshpande, S. Mehta, G.N. Jazar, Optimization of secondary suspension of piecewise linear vibration isolation systems, *International Journal of Mechanical Sciences* 48 (2006) 341–377.
[17] G.N. Jazar, R. Houim, A. Narimani, M.F. Golnaraghi, Frequency response and jump avoidance in a nonlinear passive engine mount, *Journal of Vibration and Control* 12 (2006) 1205–1237.
[18] W.J. Rugh, *Nonlinear System Theory—The Volterra/Wiener Approach*, Johns Hopkins University Press, Baltimore, MD, 1981.
[19] Z.K. Peng, Z.Q. Lang, S.A. Billings, Resonances and resonant frequencies for a class of nonlinear systems, *Journal of Sound and Vibration* 300 (2007) 993–1014.
[20] Z.K. Peng, Z.Q. Lang, S.A. Billings, G.R. Tomlinson, Comparisons between harmonic balance and nonlinear output frequency response function in nonlinear system analysis, *Journal of Sound and Vibration* 311 (2008) 56–73.
[21] Z.Q. Lang, S.A. Billings, R. Yue, J. Li, Output frequency response functions of nonlinear Volterra systems, *Automatica* 143 (2007) 805–816.
[22] Z.Q. Lang, S.A. Billings, Output frequency characteristics of nonlinear system, *International Journal of Control* 64 (1996) 1049–1067.
[23] S.A. Billings, J.C. Peyton Jones, Mapping nonlinear integro-differential equations into the frequency domain, *International Journal of Control* 52 (1990) 863–879.
[24] S.A. Billings, Z.Q. Lang, Truncation of nonlinear system expansions in the frequency domain, *International Journal of Control* 68 (1997) 1019–1042.
[25] G.R. Tomlinson, G. Manson, G.M. Lee, A simple criterion for establishing an upper limit to the harmonic excitation level of the Duffing oscillator using the Volterra series, *Journal of Sound and Vibration* 190 (1996) 751–762.
[26] A. Chatterjee, N.S. Vyas, Convergence analysis of Volterra series response of nonlinear systems subjected to harmonic excitation, *Journal of Sound and Vibration* 236 (2006) 339–358.
[27] Z.K. Peng, Z.Q. Lang, On the convergence of the Volterra-series representation of the Duffing's oscillators subjected to harmonic excitations, *Journal of Sound and Vibration* 305 (2007) 322–332.
[28] X.J. Jing, Z.A. Lang, S.A. Billings, New bound characteristics of NARX model in the frequency domain, *International Journal of Control* 80 (2007) 140–149.

[29] S Billings, Z.Q. Lang, A bound for the magnitude characteristics of nonlinear output frequency response functions. 1. Analysis and computation, *International Journal of Control* 65 (1996) 309–328.
[30] I.W. Sandberg, Bounds for discrete-time Volterra series representations, *IEEE Transactions on Circuits and Systems—I: Fundamental Theory and Applications* 46 (1999) 135–139.
[31] F. Thouverez, A new convergence criteria of Volterra series for harmonic inputs, *Proceedings of the 16th International Modal Analysis Conference*, 1998, pp. 723–727.